

Elucidating the role of residue 67 in IMP-type metallo- β -lactamase evolution

Running title: Role of residue 67 in metallo- β -lactamase evolution

Alecander E. LaCuran,^a Kevin M. Pegg,^b Eleanor M. Liu,^a Christopher R. Bethel,^c Ni Ai,^d William J. Welsh,^e Robert A. Bonomo,^{c,f} Peter Oelschlaeger^{a#}

SUPPLEMENTAL MATERIAL

Department of Pharmaceutical Sciences, College of Pharmacy, Western University of Health Sciences, Pomona, California, USA^a

Department of Biological Sciences, California State Polytechnic University, Pomona, California, USA^b

Louis Stokes Cleveland Veterans Affairs Medical Center, Cleveland, Ohio, USA^c

Pharmaceutical Informatics Institute, School of Pharmaceutical Sciences, Zhejiang University, Zhejiang 310058, P. R. China^d

Department of Pharmacology, Robert Wood Johnson Medical School, Rutgers, The State University of New Jersey and Division of Chem Informatics, Biomedical Informatics Shared Resource, Rutgers-Cancer Institute of New Jersey, Piscataway, New Jersey, USA^e

Departments of Medicine, Pharmacology, Biochemistry, and Molecular Biology & Microbiology, Case Western Reserve University, Cleveland, Ohio, USA^f

Correspondence to Peter Oelschlaeger

Email: poelschlaeger@westernu.edu

CONTENT

S2	TABLE S1 Primers used for PCR-based site-directed mutagenesis
S2	Circular Dichroism Materials & Methods
S2	Circular Dichroism Results & Discussion
S3	FIG S1 CD Spectra of the four enzymes studied
S4	FIG S2 CD Spectra and calculated fits
S4	TABLE S2 Summary of secondary structure analysis
S5	FIG S3 Thermal denaturation experiment
S5	FIG S4 Mutation frequency and amino acid variability at position 67
S6	References

TABLE S1 Primers used for PCR-based site-directed mutagenesis. Nucleotides are grouped into codons according to the reading frame of the *bla* genes. The nucleotides used to introduce mutations are underlined.

Primer	Sequence (5' to 3')
V67A For	GGG TGG GGC GTT <u>GCT</u> CCT AAA CAT GGT TG
V67A Rev	CA ACC ATG TTT AGG <u>AGC</u> AAC GCC CCA CCC
V67A ForL	GTT AAC GGG TGG GGC GTT <u>GCT</u> CCT AAA CAT GGT TTG GTG
V67A RevL	CAC CAA ACC ATG TTT AGG <u>AGC</u> AAC GCC CCA CCC GTT AAC
V67I For	GGG TGG GGC GTT <u>ATT</u> CCT AAA CAT GGT TG
V67I Rev	CA ACC ATG TTT AGG <u>AAT</u> AAC GCC CCA CCC
V67I ForL	GAA GTT AAC GGG TGG GGC GTT <u>ATT</u> CCT AAA CAT GGT TTG GTG G
V67I RevL	CCA CCA AAC CAT GTT TAG GAA <u>TAA</u> CGC CCC ACC CGT TAA CTT C
V67F For	GTT AAC GGG TGG GGC GTT <u>TTT</u> CCT AAA CAT GGT TTG G
V67F Rev	C CAA ACC ATG TTT AGG <u>AAA</u> AAC GCC CCA CCC GTT AAC

CIRCULAR DICHROISM MATERIALS & METHODS

The secondary structure and protein stability analysis by circular dichroism (CD) was performed using a Jasco J-715 spectropolarimeter (Jasco Inc., Easton, MD). The purified proteins were dialyzed against 5 mM phosphate buffered saline (PBS) (68.5 mM NaCl, 1 mM KCl, 5 mM phosphate, pH 7.0) and diluted to a concentration of 0.1 mg/ml. Three scans were taken from 260 to 185 nm in a 1.0 mm path length cell and averaged for secondary structure analysis with DichroWeb (1, 2) using the CDSSTR method (3) and reference data set 7 (4). For thermal denaturation analysis, protein samples were heated from 25 °C to 100 °C in 1 °C increments while monitoring CD ellipticity at 215 nm. To facilitate comparison, raw data were converted to fraction unfolded and analyzed using a two-state transition model (5, 6). The data shown in Fig. S3 were fitted to sigmoidal curves using Prism 6 (GraphPad Software, Inc., LaJolla, CA), yielding the melting temperatures T_m reported in Table 1 of the main text.

CIRCULAR DICHROISM RESULTS & DISCUSSION

Circular dichroism (CD) spectra of IMP-1, IMP-10, and IMP-1-V67I (Fig. S1) were superimposable and characteristic of the typical $\alpha\beta\alpha$ fold (7) common among all MBLs and comparable to those of other IMP variants (8-10). The small variances in molar ellipticity are within the experimental error of protein concentration measurements. The spectrum of IMP-1-V67A is slightly different in shape, that is, more positive at 193 nm and there is a small bump at 211 nm not observed for the other enzymes. Both features are consistent with a relatively higher α helical portion in this variant. The spectra were analyzed with DichroWeb (1, 2) and excellent fits were obtained when using the CDSSTR method (3) and reference set 7 (4) (Fig. S2). The quantitative analysis confirms that IMP-1-V67A has a relatively high α helical content and relatively low content of β strands and turns as well as unordered segments (Table S2). It is conceivable that alanine, which

has a high helix propensity (11, 12) disrupts the β hairpin loop structure and induces formation of a small α helix in L3. The fact that IMP-1-V67I shows lower α helical content and higher β strand and turn content than the other enzymes may be due to the fact that the fit was relatively poor, which is apparent from the higher NRMSD. Thermal denaturation was monitored with CD (Fig. S3) and revealed very similar melting temperatures (T_m) for all four enzymes, ranging from 67 to 72 °C (Table 1 in the main text). IMP-1-V67A deviated from the other enzymes in that its unfolding started at a higher temperature but then proceeded more rapidly, which could also be related to a slightly altered secondary structure relative to the other enzymes. Overall, all enzymes appear stable at physiological as well as the kinetic assay (30 °C) temperatures.

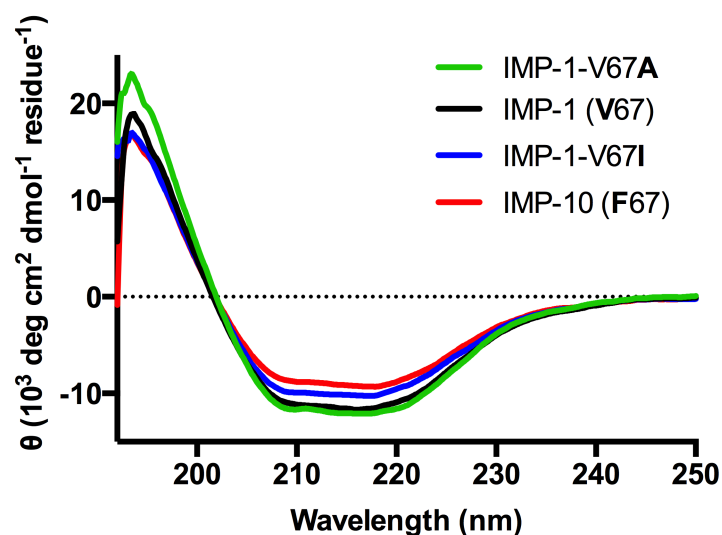


FIG S1 CD spectra of the four enzymes studied. The respective residue at position 67 for each variant is bolded in the legend.

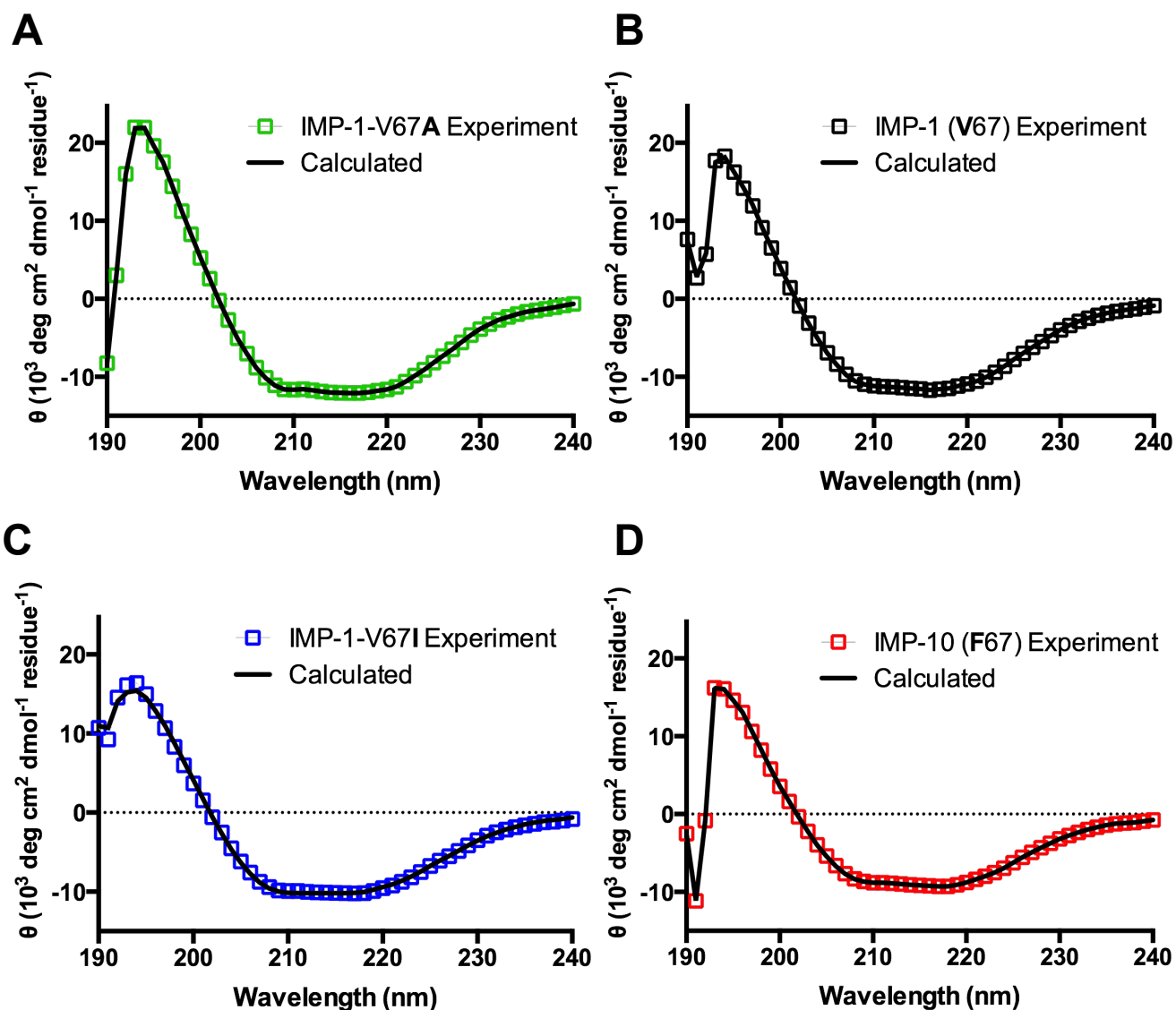


FIG S2 Experimental CD spectra (symbols colored as in FIG S1) and calculated fits that were used to determine relative content of different secondary structure elements.

TABLE S2 Summary of secondary structure element fractions of the four enzymes as determined by CD analysis from calculated fits shown in Fig. S2.

	α Helix	β Strand	Turns	Unordered	NRMSD ^a
IMP-1-V67A	0.55	0.22	0.08	0.15	0.003
IMP-1 (V67)	0.44	0.23	0.13	0.19	0.007
IMP-1-V67I	0.31	0.26	0.22	0.21	0.036
IMP-10 (F67)	0.49	0.22	0.08	0.20	0.004

^a NRMSD, normalized root-mean-square deviation

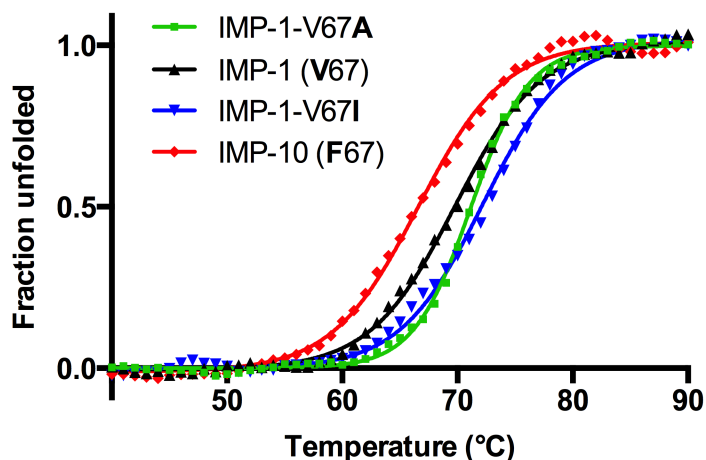


FIG S3 Thermal denaturation experiment of the four enzymes studied. Denaturation was monitored based on the CD signal at 215 nm and converted to fraction unfolded using a two-state transition model. The curves are sigmoidal fits of the resulting data.

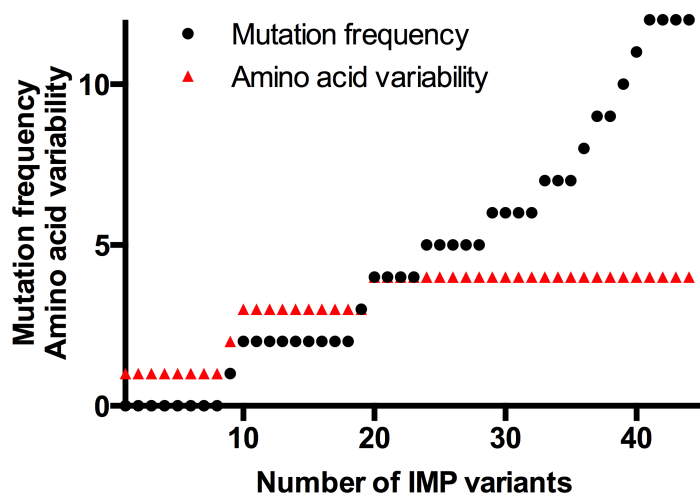


FIG S4 Frequency of mutations (relative to IMP-1) and amino acid variability at position 67 plotted *versus* the number of reported IMP variants. Note that the number of IMP variants does not correspond to the IMP-n numbering, because some variants have been assigned but not published or assigned twice.

REFERENCES

1. **Whitmore L, Wallace BA.** 2004. DICHROWEB, an online server for protein secondary structure analyses from circular dichroism spectroscopic data. *Nucleic Acids Res* **32**:W668-673. <http://dx.doi.org/10.1093/nar/gkh371>.
2. **Whitmore L, Wallace BA.** 2008. Protein secondary structure analyses from circular dichroism spectroscopy: methods and reference databases. *Biopolymers* **89**:392-400. <http://dx.doi.org/10.1002/bip.20853>.
3. **Compton LA, Johnson WC, Jr.** 1986. Analysis of protein circular dichroism spectra for secondary structure using a simple matrix multiplication. *Anal Biochem* **155**:155-167. [http://dx.doi.org/10.1016/0003-2697\(86\)90241-1](http://dx.doi.org/10.1016/0003-2697(86)90241-1).
4. **Sreerama N, Woody RW.** 2000. Estimation of protein secondary structure from circular dichroism spectra: comparison of CONTIN, SELCON, and CDSSTR methods with an expanded reference set. *Anal Biochem* **287**:252-260. <http://dx.doi.org/10.1006/abio.2000.4880>.
5. **Minor DL, Jr., Kim PS.** 1994. Measurement of the β -sheet-forming propensities of amino acids. *Nature* **367**:660-663. <http://dx.doi.org/10.1038/367660a0>.
6. **Smith CK, Withka JM, Regan L.** 1994. A thermodynamic scale for the β -sheet forming tendencies of the amino acids. *Biochemistry* **33**:5510-5517.
7. **Carfi A, Pares S, Duce E, Galleni M, Duez C, Frere JM, Dideberg O.** 1995. The 3-D structure of a zinc metallo- β -lactamase from *Bacillus cereus* reveals a new type of protein fold. *EMBO J* **14**:4914-4921.
8. **Oelschlaeger P, Mayo SL, Pleiss J.** 2005. Impact of remote mutations on metallo- β -lactamase substrate specificity: implications for the evolution of antibiotic resistance. *Protein Sci* **14**:765-774. <http://dx.doi.org/10.1110/ps.041093405>.
9. **Oelschlaeger P, Mayo SL.** 2005. Hydroxyl groups in the $\beta\beta$ sandwich of metallo- β -lactamases favor enzyme activity: a computational protein design study. *J Mol Biol* **350**:395-401. <http://dx.doi.org/10.1016/j.jmb.2005.04.044>.
10. **Pegg KM, Liu EM, George AC, LaCuran AE, Bethel CR, Bonomo RA, Oelschlaeger P.** 2014. Understanding the determinants of substrate specificity in IMP family metallo- β -lactamases: the importance of residue 262. *Protein Sci* **23**:1451-1460. <http://dx.doi.org/10.1002/pro.2530>.
11. **Bryson JW, Betz SF, Lu HS, Suich DJ, Zhou HX, O'Neil KT, DeGrado WF.** 1995. Protein design: a hierarchic approach. *Science* **270**:935-941. <http://dx.doi.org/10.1126/science.270.5238.935>.
12. **Meiler J, Mueller M, Zeidler A, Schmaeschke F.** 2001. Generation and evaluation of dimension-reduced amino acid parameter representations by artificial neural networks. *J Mol Model* **7**:360-369. <http://dx.doi.org/10.1007/s008940100038>.